Nuclear Instruments and Methods in Physics Research B 269 (2011) 20–22

Contents lists available at ScienceDirect

Nuclear Instruments and Methods in Physics Research B

journal homepage: www.elsevier.com/locate/nimb

Self-implantation energy and dose effects on Ge solid-phase epitaxial growth

B.L. Darby [a,*], B.R. Yates [a], N.G. Rudawski [a], K.S. Jones [a], A. Kontos [b]

[a] Department of Materials Science and Engineering, University of Florida, Gainesville, Fl 32611-6400, United States
[b] Varian Semiconductor Equipment Associates, Gloucester, MA 01930, United States

ARTICLE INFO

Article history:
Received 21 September 2010
Received in revised form 11 October 2010
Available online 20 October 2010

ABSTRACT

The effects of implantation energy and dose on Ge solid-phase epitaxial growth kinetics were studied using (0 0 1) Ge substrates self-implanted at energies of 20–150 keV and doses of 1×10^{14}–2×10^{15} cm^{-2}. All implants produced a continuous amorphous layer, which was crystallized by annealing at 330 °C for 22–176 min. At lower doses, the growth velocity was implant energy-independent while at higher doses the growth rate tended to decrease with decreasing implant energy. The decrease in growth velocity with energy at higher doses is discussed in terms of possible implantation-induced stresses altering growth kinetics.

Published by Elsevier B.V.

1. Introduction

Recently, Ge has received renewed interest as an alternative source/drain and channel material in complementary metal oxide semiconductor (CMOS) devices due to higher dopant activation and free carrier mobility compared to Si [1–3]. However, the knowledge base and understanding of CMOS-related processing of Ge is still relatively small compared to that of Si. Pre-amorphization using self-implantation to create a continuous amorphous (α) layer is a commonly used processing step which reduces channeling effects and results in higher activation of subsequently implanted dopants during solid-phase epitaxial growth (SPEG) [4–7]. Moreover, understanding the SPEG process is crucial to optimizing the performance of CMOS devices [8,9].

The SPEG process has been studied extensively for Si and is known to be influenced by many variables [10–21], though comparatively minimal similar research has been performed for Ge. A key difference between Ge and Si is that Ge is known to become highly porous [22–29] at doses above 4×10^{15} cm^{-2}. Such behavior suggests the atomistic nature of the α-Ge phase can be altered with dose or implant energy [30], which may possibly lead to dependence of the SPEG kinetics on self-implantation conditions, in contrast with Si where no such dependence is observed [11]. The goal of this work is to investigate the effects of implantation conditions on Ge SPEG.

2. Experimental

Two sets of (0 0 1) Ge samples with background B concentrations of 5.0×10^{17} cm^{-3} were self-implanted at room temperature using a VIISta 900XP ion-implanter. The first set of samples was implanted at a fixed energy of 150 keV with doses of 1.0×10^{14}–2.0×10^{15} cm^{-2} while the second set was implanted at a dose of either 1.0×10^{14} or 2.0×10^{15} cm^{-2} with implant energies of 20–150 keV. Samples were furnace annealed at 330 °C in N_2 ambient for times between 22 and 176 min. Cross-sectional transmission electron microscopy (XTEM) samples, prepared by focused ion beam (FIB) milling, were used to investigate the evolution of the SPEG process and provide a quantitative means of measuring the growth velocity, similarly as described elsewhere [21].

3. Results

Fig. 1 shows a sequence of XTEM micrographs depicting the growth process of a sample implanted at 90 keV to a dose of 2.0×10^{15} cm^{-2}. The as-implanted structure shown in Fig. 1(a) indicates an initial α-Ge layer 107 ± 3 nm thick. With subsequent annealing for 44, 88, and 132 min, the α-Ge layer has crystallized and reduced in thickness 66 ± 10, 36 ± 5, and 15 ± 5 nm, respectively. For some samples implanted to a dose of 2.0×10^{15} cm^{-2}, voids 3–35 nm in diameter spaced randomly a few hundred nm apart appeared just below the surface (not presented) and tended to swell the surface above the void. Thus, the α-Ge layer depths were measured in non-swelled regions to obtain the most accurate measurement of SPEG kinetics.

Fig. 2 shows the measured α-Ge layer thickness versus time behavior for samples implanted at 150 keV with doses of 1.0×10^{14}–2.0×10^{15} cm^{-2}, shown in Fig. 2(a), and for samples implanted with energies of 20–150 keV with a dose of 1.0×10^{14} or 2.0×10^{15} cm^{-2}, shown in Fig. 2(b). The average growth velocity from each set of thickness versus time data was calculated using least-squares regression analysis from 22 to 88 min as shown in Fig. 3. The linear regression analysis was performed on data from

* Corresponding author.
E-mail address: bdarby@ufi.edu (B.L. Darby).

0168-583X/$ - see front matter Published by Elsevier B.V.
doi:10.1016/j.nimb.2010.10.009

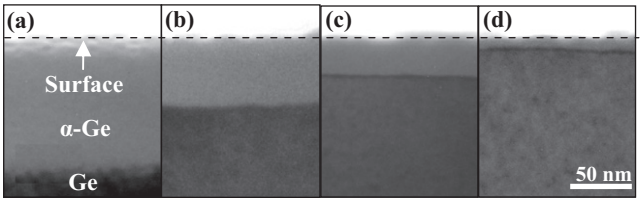

Fig. 1. XTEM micrographs of the solid-phase epitaxial growth process at 330 °C of (0 0 1) Ge self-implanted at 90 keV to a dose of 2.0×10^{15} cm^{-2}: (a) the as-implanted structure, (b) after annealing for 44 min, (c) after annealing for 88 min, and (d) after annealing for 132 min.

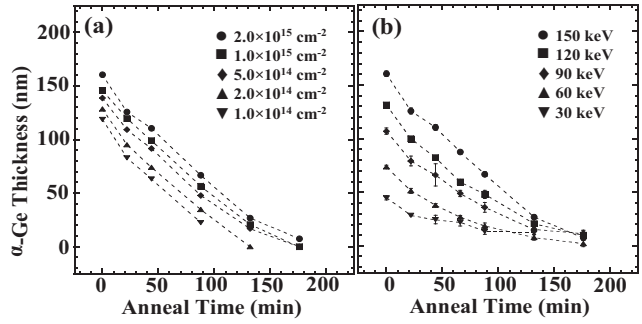

Fig. 2. Amorphous layer thickness versus annealing time behavior at 330 °C of self-implanted (0 0 1) Ge: (a) samples implanted at 150 keV with doses of 1.0×10^{14}–2.0×10^{15} cm^{-2} and (b) samples implanted with energies of 30–150 keV with a dose of 2.0×10^{15} cm^{-2}.

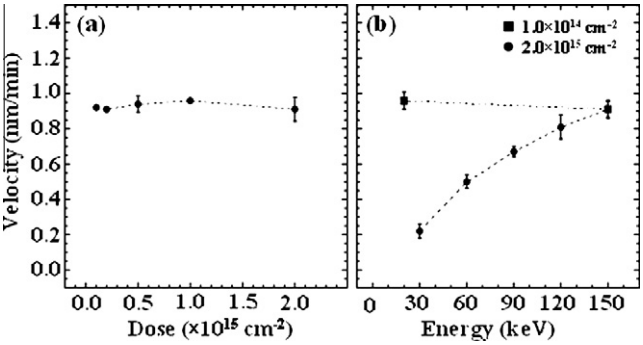

Fig. 3. The solid-phase epitaxial growth velocity at 330 °C of self-implanted (0 0 1) Ge: (a) the effect of implanted dose for samples implanted at 150 keV and (b) the effect of implant energy for samples implanted at a dose of 1.0×10^{14} or 2.0×10^{15} cm^{-2}.

22 to 88 min in order to reduce the error in SPEG velocity calculations from the initial planarization of the α/crystalline interface as well as the final crystallization near the surface. For samples implanted at 150 keV with doses of 1.0×10^{14}–2.0×10^{15} cm^{-2}, presented in Fig. 3(a), the growth velocity was nearly identical for all doses with an average growth velocity of 0.93 ± 0.02 nm/min, which agrees well with the values reported in the literature for similar implant conditions [31–33]. In terms of energy-dependence, as shown in Fig. 3(b), the growth kinetics of samples implanted at a dose of 1.0×10^{14} cm^{-2} showed little variation with energy. However, for samples implanted with a dose of 2.0×10^{15} cm^{-2}, the growth velocity clearly decreased with decreasing implant energy. This behavior differs considerably from that of self-amorphized Si, where the SPEG kinetics are independent of implantation conditions [11].

4. Discussion

It is not clear why there would be any influence of implantation conditions on SPEG kinetics for self-amorphized Ge since no such effect is observed in Si. It is known that H and/or O contamination in the near-surface region during annealing can slow SPEG [11,33–35], though the depth into which such contamination is known to occur (several hundred nm) would imply such an effect would be identical for all α-Ge layer thicknesses used in this work. For a given implant condition, the growth rate was independent of the growth interface depth [31,36] which again contradicts the notion of contamination reducing the growth velocity. Additionally, the presence of electrically-active dopants [19,20,33,37] alters growth kinetics but this effect is only observed with dopant levels 4.0×10^{18} cm^{-3}, which is much higher than the background concentrations used in this work. Also, this background concentration should be uniform throughout the wafer for all samples.

A possible explanation of the variation of SPEG with implant energy is implant-induced stress since the presence of stress at the growth interface is known to alter SPEG kinetics [9,21,38,39]. One study showed that compressive stresses in the plane of the growth interface are generated during Kr^+ – implantation into Ge, where the generated stresses increased with dose at a fixed implant energy [25]. While the implanted ion in the present study is different, a reduction of the implant energy at a fixed dose leads to a higher density of implanted ions, similarly to the previous work. Strain could be attributed to an increase in three and fivefold configurations upon implantation, leading to an increase in average bond length [40–42]. Additionally, the generation of compressive stresses resulting from implantation is consistent with current models of stress-altered SPEG [21] where in-plane compressive stresses tend to retard growth kinetics. This is further supported by the observation that growth retardation was not observed at low doses (corresponding to lower damage densities) since less stress would be generated at lower doses.

Furthermore, the structural transition of α-Ge to a porous structure at high damage densities may support the observed implantation-dependent SPEG kinetics being influenced by stress [22–29]. As stated earlier, high dose/low implant energy conditions generated sparse, but microscopic voids (a precursor to the porous structure) and possibly, these voids are preceded by smaller, submicroscopic voids. As suggested by Mayr and Averback [25], the presence of these voids is responsible for the generation of in-plane compressive stresses during implantation, and an incident ion transferring energy to the substrate over a smaller volume increases the probability of void formation. Thus, at high doses and low implant energies, the volume over which the energy is deposited decreases, resulting in a higher probability of void formation in the α-Ge network. The in-plane compressive stress generated from void formation then could possibly slow the growth kinetics in regions between voids [38].

Finally, it should be noted that in the case of group-IV semiconductors, it is known that the amorphous phase can exist in a so-called "unrelaxed" state where short-range order is not maintained and bond lengths/angles are excessively distorted [40,42–45]. Presumably, if the amorphous phase is not "relaxed" during SPEG, the nature of bond breaking/rearrangement in the growth interface, which mediates SPEG would be affected [46]. However, the relaxation of α-Ge from the unrelaxed state is expected to occur very rapidly at the thermal budget used in this work [43,45]. A structural relaxation argument also does not account for the fact that the pores and voids in Ge are highly stable upon annealing [47]. Thus, voids (and void-generated stresses) remain even after short-range order is restored and bond lengths/angles relaxed in the non-voided material.

5. Conclusion

In conclusion, the effects of implant energy and dose on SPEG of self-amorphized Ge were studied. It was shown that implant conditions generating the greatest ion density (low energy/high dose) tended to produce the greatest reductions in growth kinetics. In conjunction with the nature of α-Ge to become highly porous at high damage densities, it was postulated that the implant produced both microscopic and sub-microscopic voids, resulting in stress and altering the growth kinetics.

Acknowledgments

The authors acknowledge the Intel Corporation for funding this work and the Major Analytical Instrumentation Center at the University of Florida for use of the FIB and TEM facilities.

References

[1] D. Kuzum, A.J. Pethe, T. Krishnamohan, K.C. Saraswat, IEEE Trans. Electron. Devices 56 (4) (2009) 648–655.
[2] F. Bellenger, B. De Jaeger, C. Merckling, M. Houssa, J. Penaud, L. Nyns, E. Vrancken, M. Caymax, M. Meuris, T. Hoffmann, K. Meyer, M. Heyns, IEEE Electron. Device Lett. 31 (5) (2010) 402–404.
[3] A. Toriumi, T. Tabata, C.H. Lee, T. Nishimura, K. Kita, K. Nagashio, Microelectron. Eng. 86 (7–9) (2009) 1571–1576.
[4] A. Satta, E. Simoen, T. Janssens, T. Clarysse, B. De Jaeger, A. Benedetti, I. Hoflijk, B. Brijs, M. Meuris, W. Vandervorst, J. Electrochem. Soc. 153 (3) (2006) G229–G233.
[5] E. Simoen, A. Satta, A. D'Amore, T. Janssens, T. Clarysse, K. Martens, B. De Jaeger, A. Benedetti, I. Hoflijk, B. Brijs, M. Meuris, W. Vandervorst, Mater. Sci. Semicond. Process 9 (4–5) (2006) 634–639.
[6] A. Satta, E. Simoen, T. Clarysse, T. Janssens, A. Benedetti, B. De Jaeger, M. Meuris, W. Vandervorst, Appl. Phys. Lett. 87 (17) (2005).
[7] S. Mirabella, G. Impellizzeri, A.M. Piro, E. Bruno, M.G. Grimaldi, Appl. Phys. Lett. 92 (25) (2008).
[8] S. Morarka, N.G. Rudawski, M.E. Law, K.S. Jones, R.G. Elliman, J. Vac. Sci. Technol. B 28 (1) (2010) C1F1-C1F5.
[9] N.G. Rudawski, K.S. Jones, S. Morarka, M.E. Law, R.G. Elliman, J. Appl. Phys. 105 (8) (2009).
[10] G.L. Olson, J.A. Roth, Mater. Sci. Rep. 3 (1) (1988) 1–77.
[11] J.A. Roth, G.L. Olson, D.C. Jacobson, J.M. Poate, Appl. Phys. Lett. 57 (13) (1990) 1340–1342.
[12] J.M. Poate, S. Coffa, D.C. Jacobson, A. Polman, J.A. Roth, G.L. Olson, S. Roorda, W. Sinke, J.S. Custer, M.O. Thompson, F. Spaepen, E. Donovan, Nucl. Instrum. Meth. Phys. Res. B 55 (1–4) (1991) 533–543.
[13] L. Csepregi, E.F. Kennedy, T.J. Gallagher, J.W. Mayer, T.W. Sigmon, J. Appl. Phys. 48 (10) (1977) 4234–4240.
[14] L. Csepregi, E.F. Kennedy, J. Electrochem. Soc. 124 (8) (1977) C287–C288.
[15] E.F. Kennedy, L. Csepregi, J.W. Mayer, T.W. Sigmon, J. Appl. Phys. 48 (10) (1977) 4241–4246.
[16] L. Csepregi, E.F. Kennedy, J.W. Mayer, T.W. Sigmon, J. Appl. Phys. 49 (7) (1978) 3906–3911.
[17] W.O. Adekoya, M. Hageali, J.C. Muller, P. Siffert, J. Appl. Phys. 64 (2) (1988) 666–676.
[18] B.C. Johnson, J.C. McCallum, Phys. Rev. B 76 (4) (2007).
[19] I. Suni, G. Goltz, M.A. Nicolet, S.S. Lau, Thin Solid Films 93 (1–2) (1982) 171–178.
[20] J.S. Williams, R.G. Elliman, Phys. Rev. Lett. 51 (12) (1983) 1069–1072.
[21] N.G. Rudawski, K.S. Jones, R. Gwilliam, Mater. Sci. Eng. R – Rep. 61 (1–6) (2008) 40–58.
[22] I.H. Wilson, J. Appl. Phys. 53 (3) (1982) 1698–1705.
[23] H. Huber, W. Assmann, R. Grotzschel, H.D. Mieskes, A. Mucklich, H. Nolte, W. Prusseit, Mater. Sci. Appl. Ion Beam Tech. 248 (1997) 301–312.
[24] H. Huber, W. Assmann, S.A. Karamian, A. Mucklich, W. Prusseit, E. Gazis, R. Grotzschel, M. Kokkoris, E. Kossionidis, H.D. Mieskes, R. Vlastou, Nucl. Instrum. Meth. Phys. Res. B 122 (3) (1997) 542–546.
[25] S.G. Mayr, R.S. Averback, Phys. Rev. B 71 (13) (2005) 8.
[26] B.R. Appleton, O.W. Holland, J. Narayan, O.E. Schow, J.S. Williams, K.T. Short, E. Lawson, Appl. Phys. Lett. 41 (8) (1982) 711–712.
[27] E.M. Lawson, K.T. Short, J.S. Williams, B.R. Appleton, O.W. Holland, O.E. Schow, Nucl. Instrum. Meth. Phys. Res. 209 (1983) 303–307.
[28] O.W. Holland, B.R. Appleton, J. Narayan, J. Appl. Phys. 54 (5) (1983) 2295–2301.
[29] B.R. Appleton, O.W. Holland, D.B. Poker, J. Narayan, D. Fathy, Nucl. Instrum. Meth. Phys. Res. B 7–8 (1985) 639–644.
[30] G. Peto, J. Kanski, G. Holmen, Appl. Phys. Lett. 55 (7) (1989) 692–693.
[31] A. Claverie, S. Koffel, N. Cherkashin, G. Benassayag, P. Scheiblin, Thin Solid Films 518 (9) (2010) 2307–2313.
[32] T.E. Haynes, M.J. Antonell, C.A. Lee, K.S. Jones, Phys. Rev. B 51 (12) (1995) 7762–7771.
[33] B.C. Johnson, P. Gortmaker, J.C. McCallum, Phys. Rev. B 77 (21) (2008) 12.
[34] G.Q. Lu, E. Nygren, M.J. Aziz, J. Appl. Phys. 70 (10) (1991) 5323–5345.
[35] L. Csepregi, R.P. Kullen, J.W. Mayer, T.W. Sigmon, Solid State Commun. 21 (11) (1977) 1019–1021.
[36] P. Kringhoj, R.G. Elliman, Phys. Rev. Lett. 73 (6) (1994) 858–861.
[37] E. Simoen, A. Brugere, A. Satta, A. Firrincieli, B. Van Daele, B. Brijs, O. Richard, J. Geypen, M. Meuris, W. Vandervorst, J. Appl. Phys. 105 (9) (2009).
[38] S. Decoster, A. Vantomme, J. Phys. D – Appl. Phys. 42 (16) (2009).
[39] N.G. Rudawski, K.S. Jones, R. Gwilliam, Phys. Rev. Lett. 100 (16) (2008).
[40] C.J. Glover, M.C. Ridgway, K.M. Yu, G.J. Foran, D. Desnica-Frankovic, C. Clerc, J.L. Hansen, A. Nylandsted-Larsen, Phys. Rev. B 63 (7) (2001).
[41] M.C. Ridgway, C.J. Glover, K.M. Yu, G.J. Foran, C. Clerc, J.L. Hansen, A.N. Larsen, Phys. Rev. B 61 (19) (2000) 12586–12589.
[42] M.C. Ridgway, C.J. Glover, I.D. Desnica-Frankovic, K. Furic, K.M. Yu, G.J. Foran, C. Clerc, J.L. Hansen, A.N. Larsen, Nucl. Instrum. Meth. Phys. Res. B 175 (2001) 21–25.
[43] M.L. Theye, A. Gheorghiu, M. Gandais, S. Fisson, J. Non-Cryst. Solids 37 (3) (1980) 301–323.
[44] S. Roorda, W.C. Sinke, J.M. Poate, D.C. Jacobson, S. Dierker, B.S. Dennis, D.J. Eaglesham, F. Spaepen, P. Fuoss, Phys. Rev. B 44 (8) (1991) 3702–3725.
[45] C.E. Bouldin, R.A. Forman, M.I. Bell, E.P. Donovan, Phys. Rev. B 44 (11) (1991) 5492–5496.
[46] N.G. Rudawski, K.S. Jones, Scr. Mater. 61 (3) (2009) 327–330.
[47] L.M. Wang, R.C. Birtcher, Philos. Mag. A – Phys. Condens. Matter Struct. Defect Mech. Prop. 64 (6) (1991) 1209–1223.